Available online at www.sciencedirect.com
SCIENCE DIRECT
Icarus 171 (2004) 68–83
ICARUS
www.elsevier.com/locate/icarus

Flood-formed dunes in Athabasca Valles, Mars: morphology, modeling, and implications

Devon M. Burr [a,*], Paul A. Carling [b], Ross A. Beyer [c], Nicholas Lancaster [d,1]

[a] *USGS Astrogeology Branch, 2255 N. Gemini Dr., Flagstaff, AZ 86001, USA*
[b] *School of Geography, University of Southampton, Highfield, Southampton SO17 1BJ, UK*
[c] *Department of Planetary Sciences, The University of Arizona, 1629 E. University Blvd., Tucson, AZ 85721, USA*
[d] *Desert Research Institute, 2215 Raggio Parkway, Reno, NV 89512, USA*

Received 2 December 2003; revised 6 April 2004

Available online 11 June 2004

Abstract

Estimates of discharge for martian outflow channels have spanned orders of magnitude due in part to uncertainties in floodwater height. A methodology of estimating discharge based on bedforms would reduce some of this uncertainty. Such a methodology based on the morphology and granulometry of flood-formed ('diluvial') dunes has been developed by Carling (1996b, in: Branson, J., Brown, A.G., Gregory, K.J. (Eds.), Global Continental Changes: The Context of Palaeohydrology. Geological Society Special Publication No. 115, London, UK, 165–179) and applied to Pleistocene flood-formed dunes in Siberia. Transverse periodic dune-like bedforms in Athabasca Valles, Mars, have previously been classified both as flood-formed dunes and as antidunes. Either interpretation is important, as they both imply substantial quantities of water, but each has different hydraulic implications. We undertook photoclinometric measurements of these forms, and compared them with data from flood-formed dunes in Siberia. Our analysis of those data shows their morphology to be more consistent with dunes than antidunes, thus providing the first documentation of flood-formed dunes on Mars. Other reasoning based on context and likely hydraulics also supports the bedforms' classification as dunes. Evidence does not support the dunes being aeolian, although a conclusive determination cannot be made with present data. Given the preponderance of evidence that the features are flood-formed instead of aeolian, we applied Carling's (1996b, in: Branson, J., Brown, A.G., Gregory, K.J. (Eds.), Global Continental Changes: The Context of Palaeohydrology. Geological Society Special Publication No. 115, London, UK, 165–179) dune-flow model to derive the peak discharge of the flood flow that formed them. The resultant estimate is approximately 2×10^6 m^3/s, similar to previous estimates. The size of the Athabascan dunes' in comparison with that of terrestrial dunes suggests that these martian dunes took at least 1–2 days to grow. Their flattened morphology implies that they were formed at high subcritical flow and that the flood flow that formed them receded very quickly.

Keywords: Mars, surface; Geological processes; Surfaces, planets; Terrestrial planets

1. Introduction

Athabasca Valles are a distributary outflow channel system at the western end of the Cerberus plains (Fig. 1). The distribution of flood-formed ('diluvial') forms in scattered MOC images supports the evidence of the MOLA data that the floodwater that carved the channels emerged from one of the Cerberus Fossae (Burr et al., 2002a, 2002b). Athabasca Valles appear very young. The most recent resurfacing event down the main channel has been dated by crater counting of the channel floor as a few Ma old (Berman and Hartmann, 2002; Burr et al., 2002b; Werner et al., 2003). These ages are uncertain because many of the craters have been determined to be secondaries (McEwen et al., 2003), and the significance of age dating from counting small craters remains a subject of debate (e.g., Barlow, 2003; Bierhaus et al., 2001; McEwen et al., 2004). In addition, arguments have been presented (Malin and Edgett, 2001; Edgett and Malin, 2003) for exhumed terrain on Mars in this region, so that crater density would reflect not formation

* Corresponding author. Fax: (982)-556-7014.
E-mail address: dmburr@usgs.gov (D.M. Burr).
[1] Currently at: Earth Surface Dynamics Program, U.S. Geological Survey, MS 906, National Center, 12201 Sunrise Valley Drive, Reston, VA 20192, USA.

0019-1035/$ – see front matter
doi:10.1016/j.icarus.2004.04.013

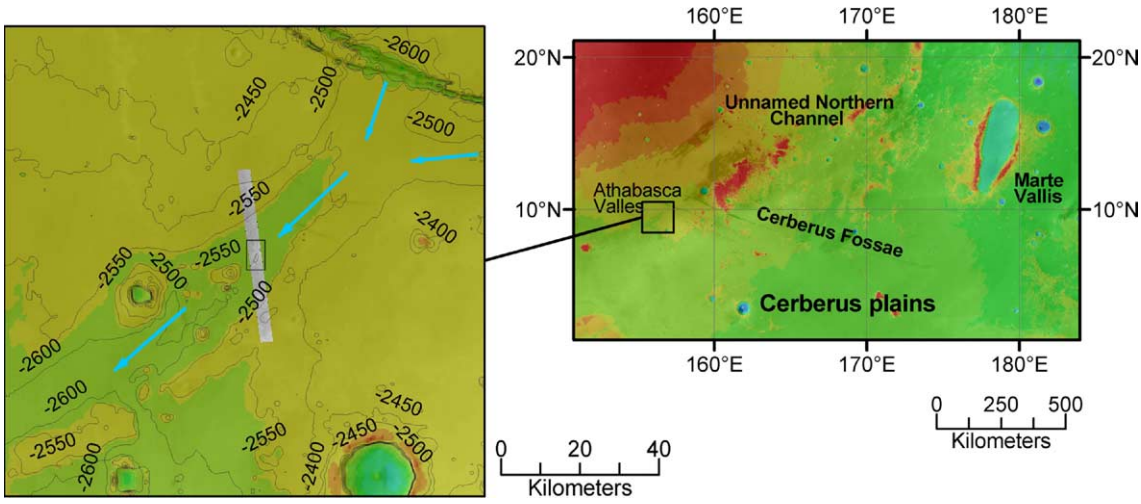

Fig. 1. Context image on right shows gridded MOLA topography of the Cerberus region overlain on MOC wide angle images. The region's three flood channels, the lava-filled Cerberus plains, and the Cerberus Fossae volcano-tectonic fissures are all indicated. Elysium Mons is to the northwest of the context image; Amazonis Planitia is to the northeast. The box indicates the upper reach of Athabasca Valles, magnified on left. The footprint of MOC image E10-01384, the location of the dunes shown in Fig. 3 (black box), and the flow direction (blue arrows) are indicated. For the electronic version of this paper, colors indicate elevations, with warm colors being high and cool colors being low. The contour interval is 50 m.

but exhumation age (but see (Berman and Hartmann, 2002, p. 10) and (Burr et al., 2002b, p. 68) for counter arguments as to why the channel terrain from which the crater counts are derived is likely not exhumed). Nonetheless, Athabasca Valles show pristine-appearing geomorphology at the resolution of MOC images, contains very few primary craters, and remains the outflow channel with the youngest model age yet derived.

Calculating the instantaneous paleodischarge down Athabasca Valles would provide clues to some important investigations on Mars. Because the floodwater was originally groundwater that emanated from the Cerberus Fossae, constraints on the floodwater paleodischarge would constrain the amount and rate of putatively recent subsurface water movement. In addition to being the source for the floodwaters, the Cerberus Fossae have also been the source for at least some of the Cerberus plains lava flows (Plescia, 1990, 2003; Keszthelyi et al., 2000; Sakimoto et al., 2001), so that constraints on the flood paleodischarge could indicate the extent of magma-groundwater/ice interactions. As life on Earth may have begun through interaction between magma and water in hydrothermal systems (summarized by Farmer, 1998), so might groundwater beneath young volcanic plains have provided the opportunity for biotic or prebiotic activity on Mars. Paleodischarge estimates would contribute information to all these investigations.

In this paper, we estimate Athabasca Valles' paleodischarge using dune-like bedforms. That is, we present data to substantiate the features' classification as subaqueous dunes created during flood flow, and we use these data to constrain the hydraulic paleodischarges associated with their development. First we summarize previous hydraulic modeling for Mars, and outline the dune-flow model we will use. Then we explain the photoclinometric technique used to derive slope and height data for the dune forms. We show morphometric similarity between terrestrial flood-formed dunes and the Athabascan features, providing the first documentation of possible diluvial dunes on Mars. We argue against the forms being antidunes, and also argue against their being aeolian. Finally, having concluded that the Athabascan features are flood-formed dunes, we apply Carling's (1996b) dune-flow model as another method for estimating paleodischarges, and outline some implications about the hydrograph (the time variation of discharge) of the flood that formed them.

2. Previous paleodischarge calculations

Paleodischarge has been estimated down Athabasca Valles (Burr et al., 2002a) with Manning's equation modified for martian gravity, i.e., $Q = (0.51/n)AR^{2/3}\Theta^{1/2}$, where Q is the discharge (m/s), n is the frictional coefficient, A is the cross-sectional area of the flow (m^2), R is the hydraulic radius (m), and Θ is the channel slope (Carr, 1979). The terrestrial Manning's equation is an empirical relationship originally derived in 1889 from work on "open channels and pipes." The frictional coefficient, Manning's n, has been derived for various types of channels (e.g., Soil Conservation Service, 1963; Hicks and Mason, 1991). With such calibration and photographic documentation of channel type, Manning's equation provides an effective method for estimating flow velocities on Earth (Chow, 1964, pp. 7–24).

Manning's equation has also been used on Mars (e.g., Smith et al., 1998). However, the application of Manning's equation to martian catastrophic floods is uncertain in the estimation of Manning's n. This derives from two factors. Firstly, the martian terrain cannot yet be seen at the same resolution as the photographs provided for calculated Manning's n (e.g., Soil Conservation Service, 1963; Hicks and Mason, 1991), hampering confident comparison to terrestrial

terrain with a known Manning's n. Secondly, the application of Manning's equation to catastrophic floods is uncertain. The Manning's n value decreases with increasing water depth (e.g., Hicks and Mason, 1991), so that Manning's n values for terrain under deep catastrophic flood flow are particularly poorly known.

The discharge down Athabasca Valles has also been estimated (Burr, 2003) with a gradually varied, step-backwater model (HEC-RAS) from the US Army Corps of Engineers (Hydrologic Engineering Center, 2001) in which the gravitational acceleration was modified for martian gravity. In common use by engineers for flood prediction, step-backwater models are also used by researchers for estimation of past terrestrial catastrophic floods (e.g., O'Connor and Webb, 1988; O'Connor, 1993; Benito, 1997). These models are an improvement over at-a-point estimates derived from Manning's equation, in that they use more complete topographic data to characterize the channel, balancing energy loss among multiple cross-sections (O'Connor and Webb, 1988). However, uncertainties remain with respect to choosing some model parameters, such as that characterizing the frictional energy losses (e.g., Manning's n) or expansion and contraction losses between channel cross-sections for deep and high-velocity floods (Carling et al., 2003). Given the uncertainties of such parameters on Earth, this type of hydraulic modeling is likely less accurate on Mars. This is both because of increased uncertainty in the selection of Manning's n values (as discussed above) and because of increased uncertainties in determining palaeoflood cross-sectional area. Flood modeling depends critically on the interpreted paleodepth of the floodwater, as well as on the amount of channel incision or infill, and these cannot be interpreted as reliably with remote sensing as for terrestrial applications. In the absence of paleoheight indicators, extraterrestrial modeling (e.g., Carr, 1979; Baker and O'Connor, 1988; Komastu and Baker, 1997; Smith et al., 1998; Burr et al., 2002a) has commonly assumed that flow in the channel is 'bankfull' (although more recent work integrated high-resolution MOC and MOLA data so as to use geologic criteria for constraining water height (Burr, 2003)). Bankfull is the flood height beyond which flood water is dispersed widely over the terrain adjacent to the channel. It is the point at which the width to depth ratio of the channel reaches a minimum (Carling, 1988), so that any modeling thus constrained results in the maximum discharge that the channel could contain. Additional uncertainty is added with the assumption that the present channel topography approximates the flood channel topography.

These modeling assumptions may be invalid for a few reasons. Catastrophic floods on Earth can both significantly erode and deposit material (Baker, 1978a), and it would be very surprising if floods on Mars did not likewise modify their channel topography. Especially in the case of multiple floods, which could effect more significant erosion than a single flood, there is no reason to expect each flood to be bankfull. Evidence of flood levels from undifferentiated multiple floods could be spatially mismatched, further distorting paleoflood height interpretation. Athabasca Valles (Burr et al., 2002b) and nearby Marte Vallis (Burr et al., 2002b; Fuller and Head, 2002) are both hypothesized to have experienced multiple floods, which would increase the likelihood of channel modification. Another modification to Athabasca Valles topography may be a shallowing of the overall channel slope, which is currently 0.0006 m/m or 0.033° (Burr et al., 2002a; Burr et al., 2002b, p. 55) possibly due to post-lava extrusion subsidence (Burr, 2003).

3. Hydraulic background

Brief definitions are here provided of hydraulic terms that will be used in later discussion. The Froude number, Fr, quantifies the criticality of the flow, and is defined as $U/\sqrt{(dg)}$, where U is the flow velocity, d is the water depth, and g is the gravitational acceleration. Flow is regarded as sub-critical when $Fr < 1.0$ and supercritical when $Fr > 1.0$. Flows with Fr values around 1.0 may be termed transitional.

As flow increases in velocity or decreases in depth, the Froude number increases. An increase in Froude number over a sedimentary bed generally results in a series of bedform transitions. First, a lower stage plane bed builds into dune bedforms. These forms then flatten into an upper stage plane bed. Finally, from this surface grow bedforms referred to as antidunes Descriptions and comparisons of dunes and antidunes are provided in Section 7: *Similarity with terrestrial diluvial dunes*, below.

Thus, Froude number values provide an approximate, semi-quantitative guide to the relationship between bedforms and flow conditions. Sub-critical flows with $\sim 0.5 < Fr \lesssim 0.84$ may contain dunes. For transitional conditions with $Fr \gtrsim 0.84$, dunes tend to diminish in height and may be washed out completely to be replaced by an upper stage flat bed or antidunes. For supercritical flow ($Fr > 1.0$), usually only a flat bed or antidunes are observed. For a more complete explanation, see Simons et al. (1965) and Carling (1999).

4. The model used in this work

In view of the uncertainties discussed above, a method for estimating discharge that is both independent of the present channel topography and does not require assuming or determining floodwater height is desirable. A model based on paleobedforms that links their morphology to the discharge that formed them is one such method. Carling (1996b) developed a model to estimate flow velocity and depth based on hundred-meter-scale transverse periodic bedforms ("dunes," cf. Ashley, 1990). Diluvial dunes are found in catastrophic flood terrains on Earth. For example, dunes are found in the Channeled Scabland of Washington state, USA, formed by Pleistocene-age catastrophic flooding from glacial Lake

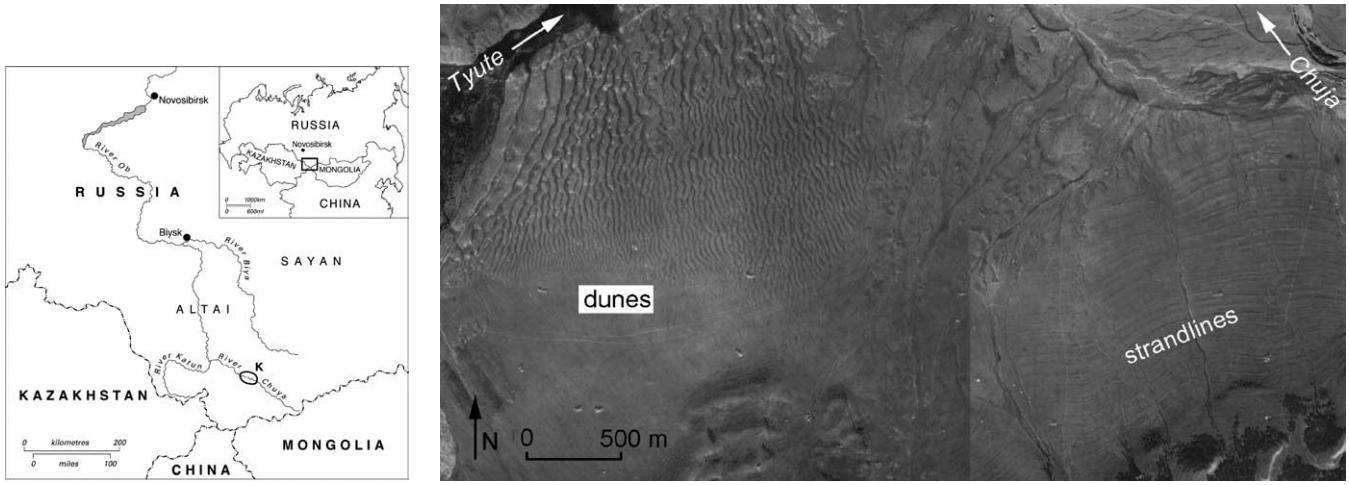

Fig. 2. Aerial photograph showing a portion of the Kuray, Siberia, dunes. (The area covered by the aerial photograph is located near the letter '**K**' in the context sketch map.) The Kuray dunes are low-amplitude (height < 16 m; length < 200 m), gravel (max sediment size < 0.2–0.5 m), transverse ridges which extend patchily over a 24-km tract. This photo shows the easterly portion of that tract, which consists of a former lake bed (hence the strandlines in the right of the image) where the sediment has accumulated in well-defined dunes. Paleoflow direction is from left to right.

Missoula (Baker, 1973), and multiple sets of diluvial dunes are also found in the Altai Mountains of south-central Siberia (Fig. 2) (Carling, 1996a; Carling et al., 2002).

Dunes transverse to the primary flow direction may be divided into those with relatively straight or gently sinuous long crestlines ("transverse ridges"), and those with long but strongly sinuous crestlines or short crestlines that are recurved with respect to the main flow ("barchanoid ridges" or "barchan dunes") (Best, 1996). For simplicity, these are termed two-dimensional (2-D) or three-dimensional (3-D) dunes, respectively, after Allen (1968) and Costello and Southard (1981). Carling's dune-flow model (Carling, 1996b) estimates depths and velocities above 2-D dunes with a force balance equation and the partitioning of flow resistance between form- and skin-drag over the dunes. We use this model in this paper and a very brief synopsis is provided here; the reader is referred to the original work for a more complete description.

The model is based on the hypothesis that the dynamics and resultant morphology of equilibrium gravel dunes in catastrophic paleoflood flow are similar to those of equilibrium dunes developed in coarse sand by fluvial bedload transport without suspension. Accordingly, equations describing bulk flow parameters over coarse sand are used, as modified for flow over gravel dunes. The modeled dune is assumed to be part of a field of dunes (i.e., an identical dune is assumed to exist upstream). Dune morphology and sediment size data are used to determine the bed roughness and shear velocity at the threshold of motion above the dune crest. This, in turn, allows the construction of a velocity profile over the crest. Velocities characteristic of the depth-averaged flow are calculated for three conditions: (1) when the dune initially grew from a lower-stage plane bed, (2) when the dune would have approached transition to an upper-stage plane bed, and (3) when the dune would have finally stabilized on a receding hydrograph. Of these three independent estimates of flow velocity, conditions (1) and (3) provide the lower probable velocities and condition (2) provides the higher possible velocity. The velocity actually represented by the dunes depends on which stage of their formation has been preserved, which must be determined by the modeler.

Carling (1996b) applied this hydraulic model to small gravel dunes in the Toutle River, Washington State and obtained reasonable agreement with measured values (Dinehart, 1992), with the greatest uncertainty associated with determinations of water depth in the model. He then used it to estimate discharge for Pleistocene-age flooding across the Kuray dune field in the Kuray basin of Siberia (Fig. 2). Results for the Siberian examples (Carling, 1996b) were of the order of 5×10^4 m^3/s for when the dunes were initiated, 7.5×10^5 m^3/s with a maximum depth of a few tens of meters for the peak flow, and 2×10^4 m^3/s for when the dunes were finally stabilized on a receding hydrograph. To date, this has been the only application of the model. These estimates are not intended to reflect a single maximum discharge, but encompass the three different stages of dune growth, and so should naturally vary somewhat.

5. Transverse dune-like bedforms in Athabasca Valles

Channel-transverse dune-like bedforms have been imaged in Athabasca Valles (Fig. 3). These forms are ten to a hundred meters in wavelength scale, sinuous or gently barchanoid in plan view. They are seen in MOC image E10-01384 (resolution 3.1 m/px), located near 9.50° N 203.85° W (approximately 156.15° E), approximately 60 km down slope from the channel's dual origination points at the Cerberus Fossae. (About the same time this work was submitted, a higher resolution image (R01-00745, 1.54 m/px) showing the dunes was released. We present our quantitative (photoclinometric) work as originally per-

Fig. 3. Subset of MOC image E10-01384, centered near 9.5° N 156.2° E, showing one transverse dune field immediately north of and contiguous to a streamlined form. Parts of two 3-D dune fields are visible farther to the north. Image resolution is 3.1 m/px; image is 3.17 km wide.

formed on the E10-01384 image. We verified our ideas qualitatively in the higher resolution R01-00745 image as noted in the text.) The dunes are contiguous to a streamlined form near the middle of the channel, although separated from that form by a narrow swath (up to ∼200 m wide) that lacks dunes (a "fosse;" see Section 7.1: *Morphology in plan view*, and Section 8.4: *Non-deposition zone*, below). Based on their similarity of form to terrestrial examples, their channel-transverse orientation, and their location in a flood channel, they have been interpreted to be subaqueous dunes (Burr et al., 2002b) or, alternatively, antidunes (Rice et al., 2002).

Two other fields of dune-like bedforms are located near the primary field. The southwestern-most tip of a second field can be seen ∼0.3 km north of the primary field; the third field is located ∼0.8 km farther north of that. In contrast to the 2-D bedforms in the southern-most field, the forms in the northern fields are short 3-D bedforms with strongly sinuous or recurved crestlines. Their disjointed

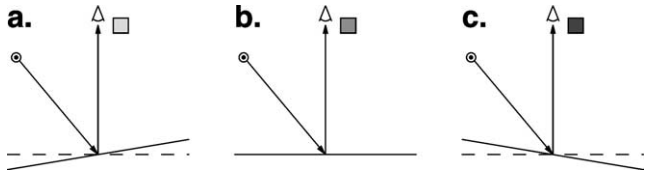

Fig. 4. Cartoon illustrating the principle behind our photoclinometry technique. The albedo varies with slope, so that the slopes angled toward the Sun appear brighter, and the slope angles away from the Sun appear darker. The bottom line represents the surface, and the color in the box is an example of the DN of a pixel taken from a surface of that slope. (a) The surface is tilted towards the Sun ('upsun'), such as the southwesterly slope of Athabascan dunes. The pixel representing that is lighter than in (b). (b) The surface is flat, such as the trough of the Athabascan dunes. The pixel representing that is of medium tone. (c) The surface is tilted away from the Sun ('downsun'), such as the northeasterly slope of Athabascan dunes. The pixel representing that is darker than in (b).

forms make them unsuitable for inclusion in the hydraulic modeling presented here, and we do not discuss them further.

6. Photoclinometry technique

For the Athabascan bedforms, the relative slopes were determined from a profiling (1-D) photoclinometry technique, which builds on the point (0-D) technique detailed in Beyer et al. (2003). The photoclinometry technique makes some assumptions about the scene in order to obtain slope estimates for each pixel. Firstly, it assumes that there is no overall tilt to the terrain. We considered this valid for this image, as the overall slope of the channel derived from gridded MOLA topography is only 0.0006 m/m (0.034°).

Secondly, photoclinometry also assumes that the surface material has a constant albedo such that small-scale brightness variations are entirely due to variations in the topography of the surface (Fig. 4). This assumption also seems reasonable. The dunes are located at the edge of a low thermal inertia (i.e., dusty) region (Mellon et al., 2000), but this dust appears in general to be evenly distributed over the dune forms that we measured, and thus would not significantly bias our measurements. The sunward facing slopes of the dunes appear as the brightest parts of the dunes, which is in accord with the image's incidence angle (43.67°). The inter-dune areas (troughs) are of a medium tone. For the upsun slope brightness to be due to dust cover, dust must have been deposited preferentially on the upsun slopes. Previous work (Thomas and Veverka, 1979; Fenton and Richardson, 2001) indicates the prevailing wind direction to be northeasterly in this region. If it were transported by the prevailing winds, any dust would thus pile up preferentially on the northeastern or downsun slopes, not the bright upsun slopes. However, dust is not moved easily by unidirectional wind flow (Greeley and Iverson, 1985, p. 253), but is instead transported by large dust storms, blanketing extensive areas rather uniformly. Thus, it is unlikely that bright dust would be preferentially blanketing one side of the dune troughs. This unlikelihood, in conjunction with

the medium tone of the dune troughs, indicates to us that this second photoclinometry assumption is valid. Isolated areas for which this assumption appears invalid, e.g., batch of dunes at the eastern edge of the image which appear to have brighter material in the troughs, were not measured. (See Section 9.2: *Infill*, for a morphologically-based estimate of other infill.)

The technique uses a lunar-Lambert photometric function to create a lookup table of the ratio of observed brightness for a range of surface slopes. It then ratios the data number (DN) values of each pixel to the average DN value for the profile and compares that directly to ratios in the lookup table to derive the slope for each pixel. The accuracy of the technique is limited by the haze in the martian atmosphere (the "haze" in the images being actually a combination of atmospheric haze and offset calibration residual in each image). One technique to correct for haze is to use the minimum pixel value in each scene as the haze value to subtract (Beyer et al., 2003). This estimate, which generally errs towards overcompensating the true haze value, would result in maximal slopes and topography. In our dune flow model, this would give a maximal model discharge. Instead, we estimated a much smaller 5% of the average DN value as attributable to haze. This amount is a more conservative estimate of the haze value than the minimum pixel value, and if less than the true haze value would result in model slopes shallower than the true slope values, and therefore more subdued topography. This would make our dune flow model results more conservative with respect to the total flow.

This profiling photoclinometry technique measures slopes most accurately in the downsun direction. In other directions, the measured slope would differ from the true slope as a function of the cosine of the angle between the downsun and the dip directions. The Athabascan transverse bedforms are generally perpendicular to the downsun direction so that with this technique, we could measure the slopes of interest directly, namely, the stoss and lee slopes of the bedforms. We made 72 measurements across roughly 45 individual forms.

We obtained estimates of bedform topography (Fig. 5b) from the slope measurements. Beginning sunward of the dune, we multiplied the image resolution by the tangent of the slope to arrive at the difference in elevation across the pixel in the downsun direction. Naturally, the errors in the elevation values build up with distance along the profile. We estimate the error in slope to be 2°–4°, and based on a 2 degree error in slope, the error in height estimates of the dune forms is $\leqslant$ 1 m (up to 50% of the height of an individual form).

7. Similarity with terrestrial diluvial dunes

In making the case for analogy between terrestrial diluvial dunes and the Athabascan features, we present quantitative morphologic similarities between the two, giving the Siberian data and then the Athabascan measurements. We find distinct dissimilarities between the Athabascan features' morphology, hydraulics, and preservation, and those of antidunes.

7.1. Morphology in plan view

The Kuray dunes (Fig. 2) are straight to slightly sinuous throughout most of the field but become more sinuous to barchanoid in the north, where they would have experienced deeper and faster flow (Carling, 1996a, pp. 651–652). Wavelengths (i.e., the distance downslope between two different dunes) range from 15 to 30 m on the south side of the dune field, and up to 200 m on the northwest side (Carling, 1996a). Where the dunes are barchanoid in the north, the spacing between dune saddles (i.e., transverse to the channel along the same dune) is generally 60–120 m (entire range is 30–150 m). (For terminology, see Fig. 5a.)

Flood-generated dunes also occur at Little Jaloman in Siberia (Carling, 1996a) where they are found within a bend in the flood channel. At this location, dunes do not develop close to the valley wall on the inside of the bend; rather there is a non-depositional flat bed zone or 'fosse' (Bretz et al., 1956) between the valley wall and the dunefield. The dunes are barchans or barchanoid towards the inside of the bend but become higher, of increased wavelength, and with more continuous crestlines towards the channel center. Such a response is usually associated with an increase in sediment supply in the deeper, faster and thus more competent flow in the channel center (Allen, 1968, 1984).

The Athabascan dune-forms are slightly sinuous to barchanoid in plan view, with a saddle-to-saddle spacing of $\sim$ 50–100 m, with an average value of $\sim$ 75 m. The wavelengths range from $\sim$ 20 to $\sim$ 135 m, with an average value of $\sim$ 60 m (Rice et al., 2002, give an average wavelength of 53.6 m). There is a distinctive fosse between the dunefield and the channel wall (Figs. 3 and 8; see Section 8.4: *Non-deposition zone* below). The fosse is most well developed immediately downstream of the crater rim's greatest extent (point S in Fig. 8) which would have been a point of flow separation in the flood flow.

7.2. Morphology in the vertical dimension

7.2.1. Slopes

The Kuray dunes have stoss slope angles of 3°–10°. The lee slope angle of the smaller Kuray dunes is as little as 3°, whereas on the larger dunes the lee slope angle is 17°–19°. (See Fig. 5a for illustration of terms.) The Kuray dunes of all sizes show a definite tendency toward asymmetry with $\sim$ 85% of the dunes having longer stoss sides than lee sides (Fig. 6).

The Athabascan features display stoss slope angles ranging from 4°–14° and lee slope angles ranging between 8°–20°. Like the Kuray dunes, they also show strong tendency toward asymmetry with $\sim$ 90% having longer stoss sides than lee sides (Figs. 5b and 6).

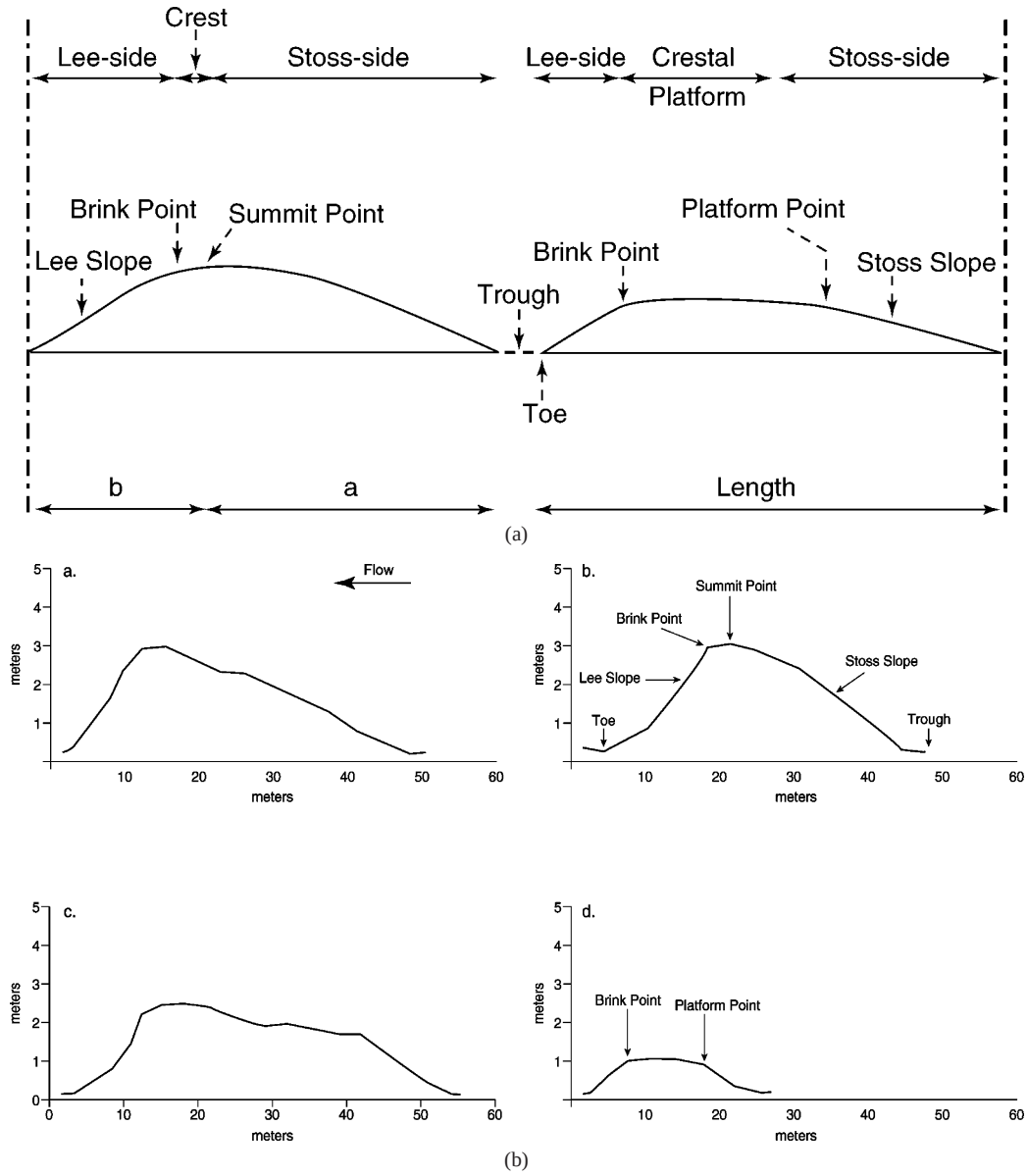

Fig. 5. (a) Definition diagram for terms pertaining to dune morphology (modified from Carling, 1996b). Flow direction is from right to left. (b) Exemplary profiles obtained using photoclinometry of the Athabascan dune forms. Vertical exaggeration is ∼ 5×. a. and b. are steep asymmetric dunes with distinctive summits and brink points. c. and d. show degrees of crestal flattening such that a near-horizontal or low gradient platform is present between the platform point and the brink point.

This asymmetry is characteristic of dunes. Dunes move downstream primarily through tractive entrainment of sediment from their stoss sides. Deposition of sediment on their lee sides often occurs by avalanching, in which material spills over the crests of the dunes and is deposited close to the angle of repose (∼ 32°). For a broad range of sediment sizes, this movement may also occur through deposition from bedload sheets (e.g., Whiting et al., 1988). Bedload sheets move over the underlying bedforms as coherent groups of fast moving layers of mobile grains, which move much faster than the dunes. As such, the bedload sheet grains run-out farther than avalanching grains and so tend to reduce the leeside angles to less than the angle of repose. This mechanism is believed to have predominated in the case of the Kuray dunes (Carling, 1996a). Despite the importance of this latter mechanism, however, the lee sides of dunes still tend to be steeper than the stoss sides, which form through the (slower) movement of sediment up the stoss slope against gravity. Thus, the majority of dunes are asymmetric, with shallower stoss slopes and steeper lee slopes (e.g., Yalin, 1977, p. 209, Fig. 7.1).

7.2.2. *Height* : *length ratio*

The Kuray dunes have a maximum height of ∼ 16 m and a maximum length of 200 m. The Athabascan forms have a maximum height of just over 5 m (the large majority are under ∼ 3.5 m high; see Fig. 7) and a maximum length of ∼ 130 m. Both sets of dune-forms show a similar maximum

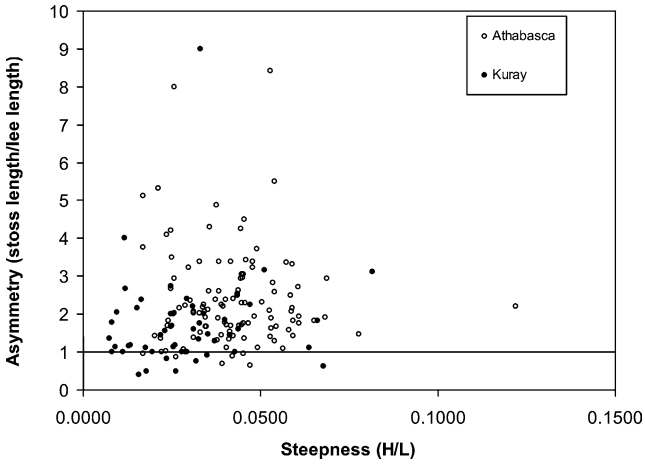

Fig. 6. Asymmetry plots for the Kuray dunes and the Athabascan features. The plot shows a similar scatter distribution of asymmetry and steepness for both sets of bedforms, and a similar percentage of points having longer stoss sides than lee sides. This asymmetry and scattered distribution is characteristic of subaqueous dunes.

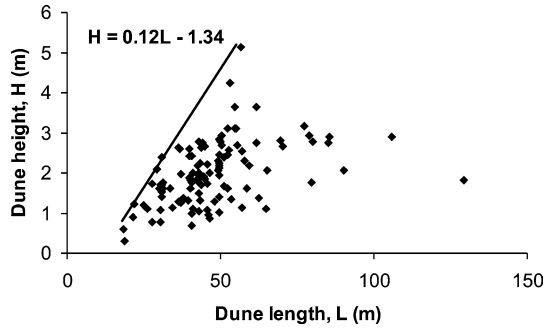

Fig. 7. Measurements of the Athabascan features, with the limiting $H : L$ ratio shown by the straight line slope. The limiting slope value of 0.12 is characteristic of subaqueous dunes.

ratio of height to length ($H : L$) (Fig. 7). A number of laboratory studies (e.g., Engelund and Hansen, 1966; Bridge, 1982; Allen, 1984; Carling, 1990) have shown that as flow strength increases, dunes grow in height up to the transition to upper-stage plane bed, at which point they begin to lose height. This behavior results in bell-shaped plots of $H : L$ as current speed increases (e.g., Carling, 1999). Thus dune $H : L$ is an indication of the stage of dune development. A number of field investigations (summarized by Ashley, 1990) have shown that dunes reach a maximum value of $H : L$ when developing in steady flow at which time they are considered to be in 'equilibrium' with the flow. For dunes in the range of 10 m high and 100 m long, this ratio is around 0.08 to 0.12, with the value decreasing for longer wavelength dunes, as calculated using the limiting equation from (Ashley, 1990, Fig. 9A). The $H : L$ ratio for the steepest of the Kuray and the Athabascan dunes approaches ~ 0.12 (Fig. 7). Thus, it may be concluded that not only had some of the martian dunes reached a maximum steepness but also they were probably in equilibrium with the formative flow.

Both sets of dune forms also show a wide range of $H : L$ ratios, apparent in the scatter of data points (Figs. 6 and 7). This is characteristic of dunes, which form and reform relatively slowly in response to changing hydraulic conditions and so display a range of asymmetries (Carling, 1996a). With an average $H : L$ ratio of 0.029, the Kuray dunes have a standard deviation of 0.016. With an average $H : L$ ratio of 0.055, the Athabascan features have (coincidentally) the same value for the standard deviation.

7.3. Counter-indications of antidune classification

In contrast to the evidence of dune classification, our analyses show little hydraulic, preservational, or morphological support for the Athabascan features' classification as antidunes (Rice et al., 2002). Dunes form during subcritical flow (i.e., Froude numbers less than ~ 0.84; Carling, 1999). This dune:antidune threshold value is theoretical and can be reduced in deep flows (Carling and Shvidchenko, 2002); yet there are no theoretical or empirical arguments for antidunes to develop in flows with Froude numbers as low as those associated with peak flow depths in the Athabascan flood model of Burr (2003), i.e., 0.3 to 0.5. Although this would not preclude antidunes developing on other flood stages when the water depth was lower (i.e., the Froude number was higher), the gentle channel gradient is not conducive to the development of transitional or supercritical flow at any flood stage.

A more compelling argument is based on preservation potential. Antidunes are transitory, usually persisting for tens of seconds and only in restricted parts of the flow that are transitional or supercritical (Reid and Frostick, 1987). On Earth, antidune morphology is rarely preserved following natural floods with extended recession limbs; preservation seems to require a very rapid recession of the hydrograph to prevent washout (Shaw and Kellerhals, 1977; Alexander and Fielding, 1997). In both of these terrestrial examples, the amplitude of the preserved antidunes was muted and only a couple of individual bedforms were preserved from inferred trains of many antidunes. This poor preservation is in clear contrast to the many preserved terrestrial dune fields in Siberia and the Channeled Scabland, and to the excellent, distinct preservation of the Athabascan bedform train both in plan and in section (Figs. 3 and 5b).

Most compelling are arguments based on morphology. Whereas dunes are commonly asymmetric with lee sides steeper than the stoss sides, antidunes in contrast are usually symmetric (Allen, 1968, 1984; Yalin, 1977) or are frequently steeper on the stoss side than the lee side (Pettijohn et al., 1987, pp. 228–229; Alexander and Fielding, 1997). This contrast results from the distinct difference between the flow conditions above dunes and those above antidunes, specifically, the phase difference between surface water waves and the bed undulations. For dunes, the water surface is out of phase with the bed, the flow is steady, and the water surface does not interact significantly with the bedform crest. For antidunes, the water surface is in phase with the bed, the flow is unsteady, and there is significant interaction between water

surface and the bed such that bedforms build and collapse repeatedly (e.g., Allen, 1984, p. 285). Although the occasional development of an antidune with an asymmetry similar to that of a dune is not precluded in nature, the authors know of no field reports of antidune trains wherein the majority of the bedforms display dune-like asymmetries.

Flow separation is a condition whereby the main current in a flow separates from the bed or channel bank, usually at a location where there is a sharp reentrant in the bed or bank profile. Within the reentrant, the flow is very turbulent and often a re-circulating flow cell develops. Such recirculating cells may often occur in the lee side of dunes because the flow separates in the region of the dune crest or brink point. Allen (1980, p. 309) and others suggest intermittent flow separation occurs when the lee slopes of bedforms are at least 5° to 9°. Permanent separation is observed around 10° to 15° (Zilker et al., 1977; Zilker and Hanratty, 1979; Ruck and Makiola, 1990; Best and Kostaschuk, 2002). Given that the lee side angles for the Athabascan bedforms are in the range 8°–20°, it is reasonable to conclude that persistent separated flow occurred in the lee of many, if not all, of the Athabascan bedforms. Such a conclusion is inconsistent with an antidune hypothesis because, as summarized by Allen (1984, p. 275), flow separation above antidunes is absent or weak, and time-averaged flow lines deform smoothly around the bedforms (Kennedy, 1961; Engelund and Hansen, 1966). Rather, the large majority of the Athabascan features, like the Kuray bedforms, display asymmetries and leeside angles consistent with a dune interpretation.

The variance in the $H : L$ ratio for groups of antidunes within any one bedform train is slight as the antidunes in general all form roughly at the same time (Allen, 1984, p. 413). This is in contrast to the Athabascan features, which show a wide $H : L$ variance (Fig. 7), with the same standard deviation as that of the Kuray dunes.

Flume and field studies show that some antidunes within individual trains, usually those in the faster flows, develop 3-D morphologies. In plan, these 3-D forms appear as distinctive *en echelon* ellipsoidal mounds and hollows, which are much more common for antidunes than 2-D geometries (Allen, 1968). These distinctive 3-D bedforms are not seen in the primary field of bedforms in Athabasca Valles, where the forms are predominately 2-D.

On the basis of their preservation, the hydraulics likely associated with their formation, and the morphology derived from our photoclinometric measurements, we conclude that the Athabascan bedforms, like those in Siberia, are dunes and not antidunes.

8. Evidence regarding a possible aeolian origin of the Athabascan dunes

When viewed in plan, aeolian transverse dunes can have very similar appearance to subaqueous transverse dunes,

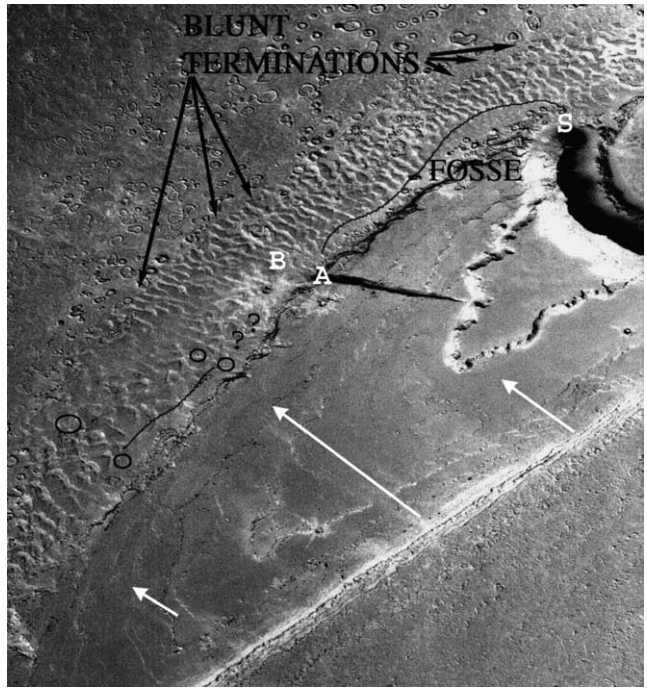

Fig. 8. MOC image of dunes in Athabasca Valles, annotated to show features discussed in Sections 7 and 8 above. The fosse is outlined by the thin black line. The black arrows point out the general location of bluntly and concordantly terminated dunes. The white arrows lie parallel to bright wind streaks. The black circles surround possible ∼ 5–9 m boulders. See text for discussion of points A, B, and S.

including linear, sinuous and barchanoid morphologies (Greeley and Iverson, 1985, p. 163). For example, Carling (1996a, p. 654) notes the consistent wavelength to transverse span ($L : W$) ratios reported for both aeolian and flood-formed barchanoid dunes. The same conclusion applies to dunes viewed in section. That is, aeolian and diluvial dunes may have similar $H : L$ ratios (Ashley, 1990, Fig. 9B) and asymmetries.

This applies to the Athabascan dunes. The sizes of terrestrial aeolian dunes include the size of the Athabascan dunes (Greeley and Iverson, 1985), and the reported height of most terrestrial aeolian dunes with a wavelength spacing of less than 100 m is less than 5 m (Lancaster, 1995), consistent with the Athabascan dune measurements. Thus the size and shape of the Athabasca dunes are not uniquely diagnostic of their origins; they could be aeolian dunes. However, other characteristics (annotated on Fig. 8) do help in determining which fluid—air or water—formed them. We discuss seven other characteristics of the Athabascan dunes, and conclude that, although not all of the characteristics are conclusive, the preponderance of them indicates the dunes to be flood-formed.

8.1. Flattening

The Athabasca dunes in general appear distinctly flattened, both in Fig. 3 (especially noticeable farther downstream, i.e., in the lower left of the image) and in photocli-

nometry profiles (Figs. 5b, 5c, and 5d). Flattening can occur in either aqueous or aeolian processes. In water flow, flattening can result from depth limitation, i.e., the water depth does not permit greater dune growth. Individual MOLA points show that the dunes sit 40–50 m below the top of the streamlined form next to it, forms that have been hypothesized (Burr et al., 2002a, 2002b; Burr, 2003) to have formed from deposition of sediment from the flood water. If this hypothesis is correct and the dunes and the streamlined form developed during the same flow, then the dunes, sitting several tens of meters below the flood's peak height, would not have been flattened due to depth limitation during peak flows. Fluvial flattening can also result from transition to an upper stage plane bed at transcritical flow (i.e., Froude numbers $\sim$ 0.84–1.2). However, the dunes, if diluvial, would have formed at subcritical Froude numbers; likewise, previous computer modeling calculated significantly subcritical flow (Froude numbers 0.3–0.5) (Burr, 2003). Lastly, dunes may also be flattened as a result of transition to a lower stage plane bed during receding flow, i.e., wash out. Crestal flattening of the Siberian dunes is attributed to this cause (Carling, 1996a), and this appears the most reasonable cause for the observed flattened crestal platforms of the Athabascan dunes.

Aeolian dunes can likewise display crestal flattening. This has been attributed to coarse grain size (Tsoar, 1986) and/or strong winds (Lancaster, 1985). Sustained strong winds do not appear characteristic of the present day martian environment (Sullivan et al., 2000). However, martian dune sand is slightly coarser than terrestrial dune sand (Edgett and Christensen, 1991), and the flattened crestal platforms could have been formed in significantly coarser sediment under a paleowind regime.

8.2. Wind streaks

Wind streaks are patterns of contrasting albedo that result from aeolian processes (Greeley and Iverson, 1985, p. 209). We observe bright wind streaks oriented ESE-WNW across the image that appear to originate at scarps along the streamlined form (Fig. 8). They are at a similar angle to low-thermal inertia swaths of secondary craters that trend southeast-northwest across Athabasca Valles (McEwen et al., 2003), but can be distinguished from them on THEMIS IR images as not being located within a secondary swath (see, for example, image I04133003, available at http://themis-data.asu.edu). These wind streaks indicate a present wind direction from the east-southeast, almost at right angles to that which would be consistent with the formation of the Athabascan dunes by wind. However, previous research (Thomas and Veverka, 1979; Fenton and Richardson, 2001) indicates that recent wind flow was northeast to southwest, which would be consistent with the dunes' formation by wind. Thus, the dunes' orientation indicates that either they are not aeolian or, if they are aeolian, they formed under a recent paleowind regime.

8.3. Grain size

The grain size of the sediment in the dunes would be the clearest indication of whether they were formed by wind or by water. Although the size of grains transported in catastrophic floods cannot be calculated analytically, deposits from terrestrial catastrophic floods with estimated discharges on the order of $1–10 \times 10^6$ m^3/s contain sediment of boulder-size (O'Connor, 1993), including boulders several meters in diameter (e.g., Baker, 1978a, p. 71). The lower gravity on Mars would result in slower water flow and therefore a smaller sized grain that could be transported, but it also decreases the weight of the rock. So the net effect of Mars' lower gravity is to increase the transport competence for a given water flow by a factor of a several (for the smallest grains) to a factor of $\sim$ 1.6 (for the largest grains up to 10 cm in diameter) (factors estimated from Komar, 1980, Fig. 1 and Table 1). Thus, martian flood flow on the order of $\sim 1 \times 10^6$ m^3/s might be expected to have transported grains of a size similar to those found in terrestrial flood deposits, i.e., boulders a few meters in diameter, if such sediment were available. The basalt proposed to dominate the terrain surrounding Athabasca Valles may well provide sediment of such size, as the Yakima Basalt of the Columbia River Basalt Group provided to the Channeled Scabland flood (Baker, 1978a).

In contrast, wind on Mars, because of the low atmospheric density, must be considerably stronger than winds on Earth to transport the same sized grains (Greeley and Iverson, 1985, pp. 68–70). Aeolian dunes on Mars have been shown to be composed of medium to coarse sand with grain size on the order of a few hundred microns (Edgett and Christensen, 1991). Wind sorts sediment well, so that it is unlikely to find grains much larger than several hundred microns in martian aeolian dunes.

Thus, the presence of boulders in the Athabasca dunes would indicate their formation by catastrophic flood flow, unless those boulders were protruding from the channel floor below the dunes. A few clusters of 3 to 6 pixels on the higher resolution R01-00745 MOC image look boulder-like, being brighter on their sunward sides and darker on their downsun sides (Fig. 8). If these clusters of pixels are boulders, they would be approximately 5–9 m in diameter. This would be clearly too large for them to be aeolian sediment, but a reasonable size for diluvially transported boulders. However, we could not make a conclusive determination of those possible pixel clusters as boulders. Thermal inertia calculations, by providing constrains on the dunes' average grain size, would help suggest which fluid formed them; such work is in progress.

8.4. Non-deposition zone

A thin swath of channel floor lacking dunes separates the streamlined form and the dune field immediately to its north (Fig. 8). In the Channeled Scabland, such a zone of non-

deposition between diluvial bedforms (e.g., dune-covered bars) and the channel wall has been termed a "fosse" (Bretz et al., 1956, pp. 977–979, Plate 8). Similar non-depositional zones forming hollows between bedforms and the valley wall have been described and latterly modeled by Carling (1987, 1989) who attributed them to flow separation immediately downstream of a flow expansion or channel bend. This subaqueous interpretation appears consistent with the Athabascan dunes. The dunes pattern shows that deposition diminished immediately downslope of the eroded impact crater, where the outward momentum around the crater would have caused the flow to separate from the streamlined form wall (point S in Fig. 8). Dune deposition then occurred progressively closer to the bar a few hundred meters further downslope, but is obscured either by outwash from the dark fissure in the streamlined form (point A), or by ejecta from the crater (point B in Fig. 8) which appears from its lighter color to be one of the multiple secondary craters in this channel (McEwen et al., 2003). A further poorly defined zone of non-deposition can be traced downslope along the side of the valley wall.

Such distinctive longitudinal zones of non-deposition are generally not seen in aeolian dune fields, due to the more diffuse nature of aeolian sediment transport. Wind flow transporting sediment in a direction perpendicular to a cliff or other obstacle can result vortex return-flow from the obstacle and in a band of non-deposition between the obstacle and the associated echo dune ("moat," Greeley and Iverson, 1985). For the formation of such a moat, however, the dune should be oriented approximately normal (traveling perpendicular) to the obstacle, whereas the Athabascan dunes are oriented perpendicular to the edge of the streamlined form.

8.5. Blunt, concordant termination of outer tips of dunes

The spanwise ends of dune crestlines are usually termed 'defects' or 'terminations' (Anderson and McDonald, 1990; Werner and Kocurek, 1997, 1999). The outer (i.e., away from the streamlined form) terminations are remarkably concordant or aligned with each other and blunt with a squarish appearance (Fig. 8). These blunt, concordant terminations suggest sedimentation which is controlled by topography, i.e., subaqueous sedimentation in which the flow is channelized. In contrast, aeolian dunes if linear generally display more pointed tips (e.g., Wilson et al., 2003, Fig. 5), or if barchans do not show alignment of the terminations or the saddles (e.g., image 23a and b in Edgett and Malin, 2000).

8.6. Contiguity of dune field to streamlined form

The Athabascan dune field hugs the curve of the northern side of the streamlined form. This is characteristic of diluvial dunes, which are closely controlled by topography and flow obstacles. In contrast, aeolian dune fields tend more towards the formation of broad flat sheets (e.g., Breed et al., 1987) unless topographically confined as within a crater (Malin and Edgett, 2001, pp. 23495–23496). The narrow, contiguous form of the Athabascan dune field with no confinement on its northern side indicates formation by a fluid that was significantly controlled by the topography, i.e., water.

8.7. Albedo

The Athabascan dunes are of a moderate albedo similar to both the channel floor and the adjacent streamlined form. This departs from the very broad classification of aeolian dunes as dark-toned and from the commonly observed contrast between wind-transported sediment and the more solid surface on which it lies (Malin and Edgett, 2001). The similarity of albedo suggests a similarity of size and/or composition for the material comprising the dunes, the channel floor on which it rests, and the streamlined form. This may be a result of the three surfaces all being comprised of diluvial sediment.

In summary, the dunes' morphology and flat tops are consistent with either aeolian or diluvial formation. The flattening of the dunes and their orientation at right angles to visible wind streaks indicate that if they are aeolian, they were formed in a paleowind regime. Definitive information on grain size is lacking. The fosse, the blunt concordant outer terminations of the dunes, the dunes' contiguity to the streamlined form and their albedo appear more consistent with subaqueous formation. We conclude from this evidence that the dunes are diluvial.

9. Other considerations

Here we discuss two other considerations that impact our analysis of the dunes as diluvial bedforms: (1) the possibility that the dunes formed not during continual channelized flood flow, but during a sudden efflux of slow moving or stagnant ponded water, and (2) the amount of dust infill.

9.1. Possible formation of the dunes in ponded water efflux

Diluvial dunes can be created in catastrophic release of ponded water. Dunes in glacial Lake Missoula were one of the primary indications of the catastrophic water efflux from the lake (Pardee, 1942), which led to the carving of the Channeled Scablands (Baker, 1978b). Likewise, some of the Siberian dunes are thought to have resulted from strong currents generated during outflow from a glacial lake as determined from ground penetrating radar (Carling et al., 2002, p. 24). Such a scenario is possible for the Athabascan dunes as well, as they sit at the upslope end of a reach of channel hypothesized to have been a site of temporary ponding (Burr, 2003, p. 661–662), but we have no way to asses this possibility remotely. If the dunes did form during ponded water efflux, the modeling presented here would reflect only the magnitude of that efflux and not a flood emanating from the Fossae.

9.2. Infill

The troughs of diluvial dunes on Earth, commonly resulting from flooding associated with glaciation, are often filled in with glacial flour or loess. For example, the topography of the Siberian dunes is subdued by 0.8 to 1.7 m of post-flood loess in their troughs (Carling, 1996a, p. 654). The western Cerberus plains region of Mars is characterized in Thermal Emission Spectrometer data by low thermal inertia, which is indicative of small grain sizes (Mellon et al., 2000). Thus, the Athabasca dunes may also have been in-filled with aeolian sediment subsequent to their formation.

We discussed above (Section 6: *Photoclinometry technique*) why we conclude that bright dust infill is photometrically insignificant to our argument that the forms are dunes, which is based in large part on their relative slopes. Here we estimate any post-flood infill through comparison to terrestrial dune morphology. Empirical data show that terrestrial dunes generally cluster below a maximum $H : L$ ratio (Ashley, 1990) indicative of dunes being 'equilibrium' adjustments of the deformable bed to the imposed flow. Dunes falling substantially above or below this ratio can be regarded as non-equilibrium (Carling, 1996b); for example, dunes with larger ratio values are "over-steepened" and hydrodynamically unstable. For a plot of ~ 425 terrestrial gravel dunes, only 12 points (i.e., $\sim 3\%$) exceed the limit line for the $H : L$ ratio for equilibrium dunes (the $H : L$ limit line, but not the terrestrial data, is shown on Fig. 7). The Athabascan dune data ($n = 72$) also cluster below Ashley's $H : L$ limit line; only 1 point (1%) falls above that line. Subtracting a hypothesized 0.5 m of dust infilling the troughs increases the dune trough-to-crest heights, and puts 2 points (3%) above Ashley's $H : L$ ratio limit. This is an acceptable percentage, when compared with $\sim 3\%$ for terrestrial data, in excess of the equilibrium value. Subtracting a hypothesized 1 m of dust infilling the troughs puts 7 points (10%) above the $H : L$ ratio limit, which is too large a percentage in excess of the equilibrium value. We conclude that < 0.5 m of aeolian sediments have infilled the Athabascan transverse dunes. As a conservative estimate, we modified our data for 0.5 m of infill (shown as open circles on Fig. 7) and used this modified data for our modeling.

10. Modeling

The model uses sediment size information, d_{50} (the 50% grain size) and d_{84} (the 84% grain size), to calculate bed roughness and shear velocity at sediment entrainment over the dunes. This calculation in turn is used to construct a velocity profile of the flow. However, these sediment sizes could not be determined from the MOC images of the dunes. With the highest available resolution (1.54 m/px), grains (boulders) would need to be > 4.5 m in diameter to be visible. As only a few pixel clusters have the potential to be boulders, we infer that in general the sediment in the dunes consists of finer grain sizes.

In the absence of higher resolution image data, we initiated the model with flow velocities from the previous HEC-RAS modeling (Burr, 2003) in order to estimate sediment size. The HEC-RAS modeling showed velocities of 3–5 m/s. For these velocities, sediment sizes 2 mm or finer would have been transported in suspension (Komar, 1980, Fig. 2), i.e., by upward currents in turbulent flow that support the particles' weight. Sediment coarser than 2 mm would have been transported as bedload. Bedload is moved by rolling, sliding, or bouncing along the channel bottom, although some bedload sediment moves from the crest of one dune to the stoss slope of the next dune in suspension. Dunes, as bedforms, consist predominately of bedload, not suspended load. Given this predominance, Komar's calculations, and the visual hint of 5–9 m diameter boulders, we infer that the Athabascan dunes consist of sediment that at its smallest is coarser than 2 mm (i.e., gravel). Thus, we used an average dune sediment size of 3 mm ($d_{50} = 3$ mm). We further assumed that, having been deposited from catastrophic flood bedload, the dune sediment is poorly sorted (phi standard deviation $= 1.60$) such that the 84th percentile sediment diameter, d_{84}, is equal to 9 mm (Boggs, 1995, p. 89; Swan and Sandilands, 1995).

We used these sediment size percentiles to run the dune flow model. That is, we used the grain sizes along with the dune dimensions to calculate the combined grain and form roughness of the dunes and the velocity profile of the flow (see Carling, 1996a, 1996b, pp. 171–175). From that profile, we estimated the velocities associated with the three stages of dune growth, namely, initiation (with Shields' non-dimensional ratio set to 0.045), maximum development or incipient wash-out, and stabilization on a waning hydrograph. We also calculated grain and form drag friction factors, which allowed us to estimate flow depths (see Carling, 1996a, 1996b, Eqs. (13) and (15)). Our results were as follows: at dune initiation, velocity and depth were 0.42 m/s and 3.7 m; at maximum development, they were 0.86 m/s and 4.10 m; and during waning flow stabilization, they were 0.49 m/s and 2.3 m.

As per the continuity equation, discharge estimates require flow width. In the HEC-RAS modeling, flow margins were constrained in part by the boundary between the interpreted diluvially lineated terrain within the topographic (MOLA) channel and the surrounding unlineated terrain (see Burr, 2003, Fig. 2A). This boundary is visible in only a couple of MOC images near the dune field, and no MOC images show the flow margin at the channel cross-section through the dune field itself. Thus, we used the flow margin as interpolated by the HEC-RAS modeling in our discharge calculations. This modeled flow width was 18.9 km. Therefore, the discharges for the three stage of dune growth were about 2.9×10^4, 6.7×10^4, and 2.1×10^4 m^3/s, respectively.

This 3 mm grain size represents an extreme lower limit for the size of sediment that would have been transported as

bedload. And it results in model flow depths that barely exceed or fail to exceed the heights of the dunes. To encompass sediment size uncertainties, we also ran the model for a sediment size one order of magnitude larger (i.e., $d_{50} = 30$ mm, and $d_{84} = 90$ mm). Komar (1980) shows all material of this size would have been transported as bedload, and bedload transport of this size range of material is consistent with the HEC-RAS modeling of bed shear stresses. Dune flow model velocity for the three stages of dune growth with this larger grain size was 1 m/s with a depth of around 4 m, 5.5 m/s with a depth of ~ 20 m, and 3 m/s with a depth of ~ 19 m. Discharge was therefore 7.5×10^4 m^3/s for the initial formation of the dunes, 2.1×10^6 m^3/s at the dunes' maximum development, and 1.0×10^6 m^3/s at the waning stage stabilization.

These dune model discharge calculations were initiated with HEC-RAS model velocities, instead of with actual grain size data. Thus, any errors in the HEC-RAS velocity modeling, if unconstrained, would result in errors in the dune flow modeling. For example, the HEC-RAS model velocities may be too slow due to a post-flood shallowing of the channel slope (Burr, 2003, p. 662). However, we have an independent constraint on the velocity, namely, the presence of dunes.

The dunes constrain the Froude number. As discussed above (Section 3: *Hydraulic background*), $Fr = U/\sqrt{(dg)}$. Flume experiments (summarized by Guy et al., 1966) have shown that dunes are commonly associated with Froude numbers between ~ 0.5 and ~ 0.84 (upper limit as given by Carling and Shvidchenko, 2002).

The determination of the Froude number in turn constrains the velocity. The Froude number calculated from the HEC-RAS modeling was ~ 0.5. If the modeled HEC-RAS velocity were too low, then the actual Froude number would have been greater than this modeled value. This is possible, as the Froude number constrained by the presence of the dunes could have been as high as ~ 0.84. If the modeled HEC-RAS velocity were too high, then the actual Froude number would have been lower than the modeled value. This is not possible, as the modeled value is already at the lower limit for dune formation; nor, frankly, does it seem physically realistic, as the flow velocity is already quite low compared to measured velocities in terrestrial rivers (e.g., Dinehart, 1992).

As noted by Carling (1996b), the water height is the most uncertain of the parameters determined by the dune flow model. The maximum water heights calculated by the dune flow model are lower (by $\sim 50\%$) than those derived from the HEC-RAS model constrained by MOC and MOLA data. In principle, dunes can form in the deeper water flows. Uncertainty in the HEC-RAS model heights results in part from the spacing of the MOLA data points and the surety with which the geomorphology in the MOC image can be interpreted. We hold either model to be accurate only to within an order of magnitude and aim to constrain the discharge only to within that accuracy (see Carling, 1996a, 1996b). Thus, we consider the difference between their modeled water heights to be acceptable with these models. The following argument regarding the water height therefore applies to both the values of the HEC-RAS model, and the values output from the dune flow model.

We argue again on the basis of the dunes that the values for peak water depths are approximately correct. If the actual water height were higher than the model height, this would depress the actual Froude number to below ~ 0.5 (its model value). However, the dunes constrain the Froude number to $\geqslant 0.5$ up to ~ 0.84. A significantly lower actual water height also seems unlikely, because Froude numbers would be too high, i.e., greater than ~ 0.84. The longitudinal lineations used in the HEC-RAS modeling to constrain flood flow provide an indication of the minimum flood water height. That is, the peak water height must have been at least as high as the lineations, and may quite possibly have been extended some distance above them. (The water height obviously must also have been at least as high as the top of the dunes, which is lower than the longitudinal lineations' highest extent.) The dunes may have formed at a stage when the water depths were less than their maximum, as indicated by the elevational extend of the lineations; this is not inconsistent with dune and flood dynamics.

In summary, the dune flow model gives a set of peak discharge values that vary with the model grain size of the bed material. When the grain size is coarse (i.e., $d_{50} = 30$ mm), the model result is $\sim 2 \times 10^6$ m/s for stage 2 development, which is consistent with the HEC-RAS modeling. Although the dune model was initiated with velocities from the HEC-RAS model, we consider it to be independently confirmed through the hydraulic constraint imposed by the dunes. Because the channel may have been steeper during the flood flow that formed the dunes, and because the dunes may have formed at a discharge less than peak flow, we consider our discharge values to be minima.

11. Summary and implications

From an analysis of morphology, hydraulics, and preservation condition, in comparison with a terrestrial analog, we have concluded that the channel-transverse periodic bedforms in Athabasca Valles are dunes. Based on their similarity to terrestrial flood-formed dunes, and dissimilarity to terrestrial and martian aeolian dunes, we have also concluded that they were diluvially formed. This is the first documented occurrence of diluvial dunes in a martian outflow channel, and provides at least one counter example to the hypothesis from MOC and THEMIS data (Rice et al., 2002) that outflow channels on Mars lack depositional bedforms. The dunes indicate that the Froude number of the flood that formed them was ~ 0.5 to ~ 0.84. The flatness of the dunes suggests that the actual value is at the upper end of that range, whereas prior modeling (Burr, 2003) gave values as the low end of

this range. We attribute this discrepancy to uncertainties in parameterization of the two different models.

From our application of Carling's dune flow model, we have derived a set of possible discharges. The range in this set of values derives in part from three possible different stages of dune growth associated with the dune forms at (1) incipient growth, (2) near transition to an upper stage plane bed, and (3) at stabilization on the waning limb of the hydrograph. As discussed above, the Athabascan dunes are flattened, and this most reasonably resulted from incipient transition to plane bed conditions (stage (2)).

The range also derives from the use in the model of two different grain sizes. The smaller grain size represents the minimum possible value for material transported as bedload, and thus the minimum possible value for material in the dunes. It also results in model flow depths that barely exceed or fail to exceed the dune heights. The larger size is an order of magnitude increase. Inasmuch as it is not an end-member and results in more plausible flow depths in comparison to dune heights, the larger grain size represents a more likely value.

For these two most likely scenarios—the Athabascan dunes formed near transition to a plane bed, and their material is coarse—the corresponding discharge from the set of generated discharges is $\sim 2 \times 10^6$ m^3/s.

This value is very similar to both previous discharge estimates (Burr et al., 2002a; Burr, 2003). Because Athabasca Valles originate at a fissure and so were presumably fed by groundwater, surface discharge estimates must be compatible with groundwater throughflow. Discharges on this order have been difficult to equate with previous modeling of subsurface flow through a porous medium (Burr et al., 2002b; Head et al., 2003), although a model with new permeability values does provide groundwater discharges equal to these values (Manga, 2004).

The dunes allow us to make some judgments about the shape of the hydrograph of the flood that formed them. Coarse gravel dunes in the North Toutle River are recorded to have formed in 1 to 2 days (Dinehart, 1992). This represents a lower limit for the formation of the Athabascan dunes, which are about one order of magnitude larger than the Toutle River dunes, and so would have taken longer to grow. The preservation of these dunes indicates that this Athabascan flood receded quickly.

Acknowledgments

D.M.B. acknowledges support from NASA's Graduate Student Researchers Program (Grant NGT5-110) during project initiation, and the USGS Shoemaker Fellowship during manuscript preparation. We thank Trent Hare for his assistance with MOLA and MOC data coordination, and Josh Emery for helpful discussions. Thoughtful reviews by Randy Kirk and Mary Bourke improved the manuscript.

References

Alexander, J., Fielding, C., 1997. Gravel antidunes in the tropical Burdekin River, Queensland, Australia. Sedimentology 44, 327–337.

Allen, J.R.L., 1968. Current Ripples. North-Holland, Amsterdam. 433 p.

Allen, J.R.L., 1980. Sand waves: a model of origin and internal structure. Sediment. Geol. 26, 281–328.

Allen, J.R.L., 1984. Sedimentary structures: their character and physical basis. In: Developments in Sedimentology, vol. 30. Elsevier, Amsterdam. 663 p.

Anderson, R.S., McDonald, R.R., 1990. Bifurcations and terminations in eolian ripples. EOS 71, 1344.

Ashley, G.M., 1990. Classification of large-scale subaqueous bedforms: a new look at an old problem. J. Sediment. Petrol. 60 (1), 160–172.

Baker, V.R., 1973. Paleohydrology and sedimentology of lake Missoula flooding in eastern Washington. In: Special Paper, vol. 144. Geological Society of America, Boulder.

Baker, V.R., 1978a. Paleohydraulics and hydrodynamics of Scabland floods. In: Baker, V.R., Nummedal, D. (Eds.), The Channeled Scabland. NASA, Washington, DC, pp. 59–79.

Baker, V.R., 1978b. The Spokane flood controversy. In: Baker, V.R., Nummedal, D. (Eds.), The Channeled Scabland. NASA, Washington, DC, pp. 3–15.

Baker, V.R., O'Connor, J.E., 1988. Peak flows for cataclysmic floods. In: National Aeronautics and Space Administration Technical Memorandum, vol. 4041, pp. 299–301.

Barlow, N.G., 2003. Comparison of secondary crater production by martian and lunar impact craters. In: Div. Planet. Sci., 35th Meeting. Abstract 9.02.

Benito, G., 1997. Energy expenditure and geomorphic work of the cataclysmic Missoula flooding in the Columbia River gorge, USA. Earth Surf. Proc. Land. 22, 457–472.

Berman, D.C., Hartmann, W.K., 2002. Recent fluvial, volcanic, and tectonic activity on the Cerberus Plains of Mars. Icarus 159, 1–17.

Best, J., 1996. The fluid dynamics of small-scale alluvial bedforms. In: Carling, P.A., Dawson, M.D. (Eds.), Advances in Fluvial Dynamics and Stratigraphy. Wiley, Chichester, UK, pp. 67–125.

Best, J., Kostaschuk, R.A., 2002. An experimental study of turbulent flow over a low-angle dune. J. Geophys. Res. 107 (C9), 3135. doi:10.1029/2000JC000294.

Beyer, R.A., McEwen, A.S., Kirk, R.L., 2003. Meter-scale slopes of candidate MER landing sites from point photoclinometry. J. Geophys. Res. 108 (E12), 8085. doi:10.1029/2003JE002120.

Bierhaus, E.B., Chapman, C.R., Merline, W.J., Brooks, S.M., 2001. Pwyll secondaries and other small craters on Europa. Icarus 153, 264–276.

Boggs, S., 1995. Principles of Sedimentology and Stratigraphy, second ed. Prentice Hall, Englewood Cliffs, NJ. 774 p.

Breed, C.S., McCauley, J.F., Davis, P.A., 1987. Sand sheets of the eastern Sahara and ripple blankets on Mars. In: Frostick, L., Reid, I. (Eds.), Desert Sediments: Ancient and Modern. In: Geological Society Special Publication, vol. 35, pp. 337–359.

Bretz, J.H., Smith, H.T.U., Neff, G.E., 1956. Channeled Scabland of Washington: new data and interpretations. Geol. Soc. Am. Bull. 67, 957–1049.

Bridge, J.S., 1982. Bed shear stress over subaqueous dunes, and the transition to upper-stage plane beds—reply. Sedimentology 29, 744–747.

Burr, D.M., 2003. Hydraulic modeling of Athabasca Vallis Mars. Hydrol. Sci. J. 48 (4), 655–664.

Burr, D.M., McEwen, A.S., Sakimoto, S.E.H., 2002a. Recent aqueous floods from the Cerberus Fossae, Mars. Geophys. Res. Lett. 29 (1). doi:10.1029/2001GL013345.

Burr, D.M., Grier, J.A., McEwen, A.S., Keszthelyi, L.P., 2002b. Repeated aqueous flooding from the Cerberus Fossae: evidence for very recently extant, deep groundwater on Mars. Icarus 159, 53–73. doi:10.1006/icar.2002.6921.

Carling, P.A., 1987. Hydrodynamic interpretation of a boulder-berm and associated debris-torrent deposits. Geomorphology 1, 53–67.

Carling, P.A., 1988. The concept of dominant discharge applied to two gravel-bed streams in relation to channel stability thresholds. Earth Surf. Proc. Land. 13, 355–367.

Carling, P.A., 1989. Hydrodynamic models of boulder-berm deposition. Geomorphology 2, 319–340.

Carling, P.A., 1990. Particle over-passing on depth-limited gravel bars. Sedimentology 37, 345–355.

Carling, P.A., 1996a. Morphology, sedimentology and palaeohydraulic significance of large gravel dunes, Altai Mountains, Siberia. Sedimentology 43, 647–664.

Carling, P.A., 1996b. A preliminary palaeohydraulic model applied to Late-Glacial gravel dunes: Altai Mountains, Siberia. In: Branson, J., Brown, A.G., Gregory, K.J. (Eds.), Global Continental Changes: The Context of Palaeohydrology. Geological Society Special Publication No. 115, London, UK, pp. 165–179.

Carling, P.A., 1999. Subaqueous gravel dunes. J. Sediment. Res. 69 (3), 534–545.

Carling, P.A., Shvidchenko, A.B., 2002. A consideration of the dune: antidune transition in fine gravel. Sedimentology 49, 1269–1282.

Carling, P.A., Kirkbride, A.D., Parnachov, S., Borodavki, P.S., Berger, G.W., 2002. Late Quaternary catastrophic flooding in the Altai Mountains of south-central Siberia: a synoptic overview and an introduction to flood deposit sedimentology. Spec. Publs Int. Ass. Sediment. 32, 17–35.

Carling, P.A., Kidson, R., Cao, Z., Herget, J., 2003. Palaeohydraulics of extreme flood events. In: Gregory, K. (Ed.), Palaeohydrology: A Contribution to Global Change.

Carr, M.H., 1979. Formation of martian flood features by release of water from confined aquifers. J. Geophys. Res. 84 (B6), 2995–3007.

Chow, V.T. (Ed.), 1964. Handbook of Applied Hydrology. McGraw–Hill, New York.

Costello, W.R., Southard, J.B., 1981. Flume experiments on lower-regime bed forms in coarse sand. J. Sediment. Petrol. 51, 849–864.

Dinehart, R.L., 1992. Evolution of coarse gravel bedforms: field measurements at flood stage. Water Resourc. Res. 28, 2667–2689.

Edgett, K.S., Christensen, P.R., 1991. The particle size of martian aeolian dunes. J. Geophys. Res. 96 (E5), 22765–22776.

Edgett, K.S., Malin, M.C., 2000. New views of Mars eolian activity, materials and surface properties: three vignettes from the Mars Global Surveyor Mars Orbiter Camera. J. Geophys. Res. 105 (E1), 1623–1650.

Edgett, K.S., Malin, M.C., 2003. The layered upper crust of Mars: an update on MGS MOC observations after two Mars years in the mapping orbit. In: Proc. Lunar Planet. Sci. Conf. 34th. Abstract 1124.

Engelund, F., Hansen, E., 1966. Investigations of flow in alluvial streams. In: Acta Polytechnica Scandinavica, Civil Engineering and Building Construction Series, vol. 35. Finnish Academy of Technology, Copenhagen. 100 p.

Farmer, J., 1998. Thermophiles, early biosphere evolution, and the origin of life on Earth: implications for the exobiological exploration of Mars. J. Geophys. Res. 103 (E12), 28457–28461.

Fenton, L.K., Richardson, M.I., 2001. Martian surface winds: insensitivity to orbital changes and implications for aeolian processes. J. Geophys. Res. 106 (E12), 32885–32902.

Fuller, E.R., Head III, J.W., 2002. Amazonis Planitia: the role of geologically recent volcanism and sedimentation in the formation of the smoothest plains on Mars. J. Geophys. Res. 107 (E10), 5081. doi:10.1029/2002JE001842.

Greeley, R., Iverson, J.D., 1985. Wind as a Geologic Process on Earth, Mars, Venus and Titan. Cambridge Univ. Press, Oxford, UK. 333 p.

Guy, H.P., Simons, D.B., Richardson, E.V., 1966. Summary of alluvial channel data from flume experiments, U.S. Geol. Surv. Professional Paper 462-I.

Head III, J.W., Wilson, L., Mitchell, K.L., 2003. Generation of recent massive water floods at Cerberus Fossae, Mars, by dike emplacement, cryospheric cracking, and confined aquifer groundwater release. Geophys. Res. Lett. 30 (11), 1577. doi:10.1029/2003GR017135.

Hicks, D.M., Mason, P.D., 1991. Roughness Characteristics of New Zealand Rivers. Water Resources Survey. DSIR Marine and Freshwater, New Zealand.

Hydrologic Engineering Center, 2001. HEC-RAS Hydraulic Reference Manual, Version 3.0, CPD-69. U.S. Army Corps of Engineers Hydrologic Engineering Center, Davis, CA.

Kennedy J.F., 1961. Stationary Waves and Antidunes in Alluvial Channels. Report No. K11-R-2. W.M. Keck Laboraotry of Hydraulics and Water Resources, California Institute of Technology, Pasadena, CA. 146 p.

Keszthelyi, L.P., McEwen, A.S., Thordarson, Th., 2000. Terrestrial analogs and thermal models for martian flood lavas. J. Geophys. Res. 105, 15027–15049.

Komar, P.D., 1980. Modes of sediment transport in channelized water flows with ramifications to the erosion of the martian outflow channels. Icarus 42, 317–329.

Komastu, G., Baker, V.R., 1997. Paleohydrology and flood geomorphology of Ares Vallis. J. Geophys. Res. 102 (E2), 4151–4160.

Lancaster, N., 1985. Variations in wind velocity and sand transport rates on the windward flanks of desert sand dunes. Sedimentology 32, 581–593.

Lancaster, N., 1995. Geomorphology of Desert Dunes. Routledge, London. 290 p.

Malin, Edgett, 2001. Mars Global Surveyor Mars Orbiter Camera: interplanetary cruise through primary mission. J. Geophys. Res. 106 (E10), 23429–23570.

Manga, M., 2004. Martian floods at Cerberus Fossae can be produced by groundwater discharge. Geophys. Res. Lett. 31, L02702. doi:10.1029/2003GL018958.

McEwen, A.S., Turtle, E.P., Burr, D.M., Milazzo, M., Lanagan, P., Christensen, P.R., Boyce, J., The THEMIS Science Team, 2003. Discovery of a large rayed crater on Mars: implications for recent volcanic and fluvial activity and the origin of martian meteorites. In: Proc. Lunar Planet. Sci. Conf. 34th. Abstract 2040.

McEwen, A.S., Preblich, B.S., Turtle, E.P., Artemieva, N.A., Golombek, M.P., Hurst, M., Kirk, R.L., Burr, D.M., Christensen, P.R., 2004. The rayed crater Zunil and interpretations of small impact craters on Mars. Icarus. Submitted for publication.

Mellon, M.T., Jakosky, B.M., Kieffer, H.H., Christensen, P.R., 2000. High-resolution thermal inertia mapping from the Mars Global Surveyor Thermal Emission Spectrometer. Icarus 148, 437–455. doi:10.1006/icar.2000.6503.

O'Connor, J.E., 1993. Hydrology, hydraulics, and geomorphology of the Bonneville flood. Geol. Soc. Am. Spec. Paper 274.

O'Connor, J.E., Webb, R.H., 1988. Hydraulic modeling for paleoflood analysis. In: Baker, V.R., Kochel, R.C., Patton, P.C. (Eds.), Flood Geomorphology. Wiley, New York, pp. 393–402.

Pardee, J.T., 1942. Unusual currents in glacial Lake Missoula, Montana. Geol. Soc. Am. Bull. 53, 1569–1600.

Pettijohn, F.J., Potter, P.E., Siever, R., 1987. Sand and Sandstone, second ed. Springer-Verlag, New York.

Plescia, J.B., 1990. Recent flood lavas in the Elysium region of Mars. Icarus 88, 465–490.

Plescia, J.B., 2003. Cerberus Fossae, Elysium, Mars: a source for lava and water. Icarus 164, 79–95. doi:10.1016/S0019-1035(03)00139-8.

Reid, I., Frostick, L.E., 1987. Flow dynamics and suspended sediment properties in arid zone flash floods. Hydrol. Proc. 1, 239–253.

Rice Jr., J.W., Parker, T.J., Russell, A.J., Knudsen, O., 2002. Morphology of fresh outflow channel deposits on Mars. In: Proc. Lunar Planet. Sci. Conf. 33rd, pp. 393–402. Abstract 2026 [CD-ROM].

Ruck, B., Makiola, B., 1990. Flow over a single-sided backward facing step with step angle variations. In: Turner, J.T. (Ed.), Proceedings of the 3rd International Conference on Laser Anemometry. Springer-Verlag, New York, pp. 369–378.

Sakimoto, S.E.H., Riedel, S.J., Burr, D.M., 2001. Geologically recent martian volcanism and flooding in Elysium Planitia and Cerberus Rupes: plains-style eruptions and related water release? In: Geol. Soc. Am. Annual Meet. Abstracts with Programs 33 (6), A-431.

Shaw, J., Kellerhals, R., 1977. Paleohydraulic interpretations of antidunes bedforms with applications to antidunes in gravel. J. Sediment. Petrol. 47, 257–266.

Simons, D.B., Richardson, E.V., Nording, C.F., 1965. Sedimentary structures generated by flow in alluvial channels. In: Middleton, G.V. (Ed.), Primary Sedimentary Structures and Their Hydrodynamic Interpretation. In: Society of Economic Paleontologists and Mineralogists, Special Publication, vol. 12. Springer-Verlag, New York, pp. 34–52 and 253–264.

Smith, D.E., Zuber, M.T., Frey, H.V., Garvin, J.B., Head, J.W., Muhleman, D.O., Pettengill, G.H., Phillips, R.J., Solomon, S.C., Zwally, H.J., Banerdt, W.B., Duxbury, T.C., 1998. Topography of the northern hemisphere of Mars from the Mars Orbiter Laser Altimeter. Science 279, 1686–1692.

Soil Conservation Service, 1963. Guide for selecting roughness coefficient "*n*" values for channels. Compiled by: Guy B. Fasken, SCS-USDA, Lincoln, Nebraska 68508.

Sullivan, R., Greeley, R., Kraft, M., Wilson, G., Golombek, M., Herkenhoff, K., Murphy, J., Smith, P., 2000. Results of the Imager for Mars Pathfinder windsock experiment. J. Geophys. Res. 105 (E10), 24547–24562.

Swan, A.R.H., Sandilands, M., 1995. Introduction to Geological Data Analysis. Blackwell Science, Oxford. 446 p.

Thomas, P., Veverka, J., 1979. Seasonal and secular variation of wind streaks on Mars: an analysis of Mariner 9 and Viking data. J. Geophys. Res. 84, 4621–4633.

Tsoar, H., 1986. Two-dimensional analysis of dune profile and the effect of grain size on sand dune morphology. In: El-Baz, F., Hassan, M.H.A. (Eds.), Physics of Desertification. Martinus Nyhoff, Dordrecht, pp. 94–108.

Werner, B.T., Kocurek, G., 1997. Bed-form dynamics: does the tail wag the dog? Geology 25, 771–774.

Werner, B.T., Kocurek, G., 1999. Bedform spacing from defect dynamics. Geology 27, 727–730.

Werner, S.C., van Gasselt, S., Neukum, G., 2003. Continual geological activity in Athabasca Valles, Mars. J. Geophys. Res. 108 (E12), 8081. doi:10.1029/2002JE002020.

Whiting, P.J., Dietrich, W.E., Leopold, L.B., Drake, T.G., Shreve, R.L., 1988. Bedload sheets in heterogeneous sediment. Geology 16, 105–108.

Wilson, S.A., Zimbelman, J.R., Williams, S.H., 2003. Large aeolian ripples: extrapolations from Earth to Mars. In: Proc. Lunar Planet. Sci. Conf. 34th. Abstract 1862.

Yalin, M.S., 1977. Mechanics of Sediment Transport. Pergamon Press, Oxford, UK. 298 p.

Zilker, D.P., Cook, G.W., Hanratty, T.J., 1977. Influence of the amplitude of a solid wavy wall on a turbulent flow. Part 1. Non-separating flows. J. Fluid Mech. 82, 29–51.

Zilker, D.P., Hanratty, T.J., 1979. Influence of the amplitude of a solid wavy wall on a turbulent flow. Part 2. Separating flows. J. Fluid Mech. 90, 257–271.